

The influence of aluminum particle size on detonation of the aluminized explosives

Changgen Feng*, Lang Chen*, and Xinping Long*

For investigating the influences of the size of aluminum particles on the detonation performances of aluminized explosives, the metal plate acceleration tests and the cylinder tests were carried out with the aluminized explosives having aluminum particles in different size respectively. The free-surface velocities of the metal plates and the wall velocities of the cylinder were measured by a VISAR interferometer. The parameters of JWL equation of state for the detonation products for aluminized explosives were determined based on the experimental results of the cylinder tests. The two-dimensional numerical simulations of the acceleration tests were conducted. The ignition and growth reactive flow model of explosive detonation was used. By comparing the experimental and computational results, the parameters of the reaction rate equations of aluminized explosives were determined. The fraction reacted of aluminized explosives are given. The reaction conditions of the aluminum particles in different size are analyzed. The results show that the aluminum particles in small size react faster in the detonation than that of the large size aluminum particles.

Keywords aluminized explosives, detonation, non-ideal detonation, numerical simulation.

1 Introduction

For having the aluminum reaction in the detonation, the aluminized explosives are typical non-ideal explosives. The aluminum reaction is related to many factors, such as the confinement of the explosives, the size and shape of aluminum particle and the chemical component of detonation products etc. For many years, there have been many researches on the aluminum reaction in detonation^[1-6]. Because the aluminized explosives used by each researcher are different, the conclusions about the aluminum reaction in detonation are not comparable. The goal of the present research is to investigate the influences of the size of aluminum particles on the detonation reaction of aluminized explosives. The metal plate acceleration tests and the cylinder tests were

carried out with the aluminized explosives having aluminum particles in different size. The free-surface velocities of the metal plates and the wall velocities of the cylinders were measured by a VISAR interferometer. The two-dimensional numerical simulations of the detonation tests were conducted. By comparing the experimental and computational results, the parameters of the reaction rate equations of aluminized explosives and JWL equation of state for the detonation products were determined. The reaction rate and time of the aluminum particles reaction are discussed in the present paper.

2 Aluminized explosives

RDX mixed with the aluminum of average particle diameters 50 nm, 5 μ m and 50 μ m respectively were manufactured. In making the aluminized explosives with 50 nm-diameter aluminum particle, all manufacturing processes were carried out in the inert gas environment so as to prevent the aluminum oxidation. Table 1

Received : May 17, 2002

Accepted : September 20, 2002

*National Key Laboratory of Explosion and Safety Science

Beijing Institute of Technology, Beijing, 100081, China

summarizes the explosive formulations.

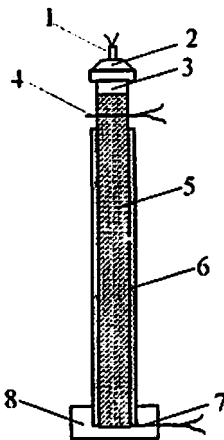
Table 1 Explosive formulations.

explosive	composition	aluminum diameter
1	RDX/Al/wax/76/20/4	50nm
2	RDX/Al/wax/76/20/4	5 μ m
3	RDX/Al/wax/76/20/4	50 μ m

3 Test facility

3.1 Cylinder test

The cylinder test is commonly used to evaluate explosive performances and to determine the parameters of the JWL equation of state of detonation products. In the present study, the cylinder tests in 25mm and 50mm diameters were carried out. Figure 1 shows the side view of the cylinder test. In 25mm cylinder tests, the cylinder expansion processes were recorded by a rotating mirror streak camera and a VISAR interferometer together. Figure 2 shows the top view of the 25mm cylinder test setup. In 50mm cylinder tests, the cylinder expansion processes are recorded by the rotating mirror streak camera only.



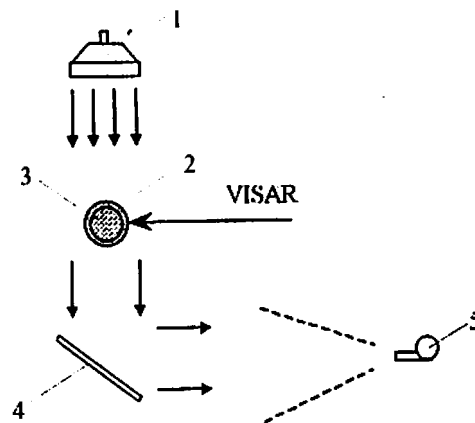
- 1. Detonator; 2. Plane wave lens 3. Booster;
- 4. Electric pin; 5. Aluminized explosives;
- 6. Copper tube; 7. Electric pin; 8. Base plate

Fig. 1 Side view of the cylinder test setup

3.2 Metal plates push test

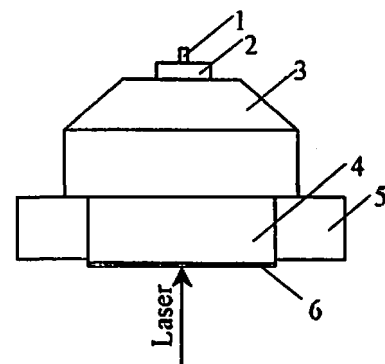
Figure 3 illustrates the setup of the metal plates push experiment setup. The detonator initiates the booster of PETN in 10mm-diameter. Then the booster initiates a plane wave lens in 42.8-diameter. The plane wave lenses generate plane shock waves

to initiate the aluminized explosives in the PMMA tubes. The sizes of the aluminized explosive pellets are 40mm in diameter with a thickness measuring 15mm. The aluminized explosives detonate and push the copper plates to move. The copper plates are 40mm in diameter with two different thickness measuring 1mm and 0.54mm. The laser beam of the VISAR interferometer irradiates the center of the copper plates vertically. The free-surface velocities of the copper plates are measured by the VISAR interferometer. Under these dimensions, the detonation behavior within the experiment timeframe of several microseconds will reach steady state and remains one-dimensional in



- 1. Explosive lens; 2. Copper tube;
- 3. Aluminized explosives; 4. Reflect Mirror;
- 5. Rotating mirror camera

Fig. 2 Top view of the 25mm cylinder test setup



- 1. Detonator; 2. Booster; 3. Plane wave lens;
- 4. Aluminized explosive;
- 5. PMMA; 6. Copper plate

Fig. 3 The metal plates push experiment setup

nature without perturbations from radial rarefactions.

4 Computational approach

A hydrodynamic code was used to simulate the metal plate push tests and the cylinder tests. The ignition and growth reactive flow model was used for the aluminized explosives⁷⁾. The product equations of state are JWL equations of state.

The following are the JWL equations of state. The Hugoniot state is described by eqn.(1)

$$p = A \left(1 - \frac{w}{R_1 V} \right) e^{-R_1 V} + B \left(1 - \frac{w}{R_2 V} \right) e^{-R_2 V} + \frac{wE}{V} \quad (1)$$

and eqn.(2) gives the Isentrope state

$$p_i = A e^{-R_1 V} + B e^{-R_2 V} + \frac{C}{V^{\omega+1}} \quad (2)$$

where, p is the pressure, V is the relative volume. A , B , C , R_1 , R_2 and ω are constants. The ignition and growth reaction rate law is of the following form

$$\frac{dF}{dt} = I(1-F)^a \left(\frac{p}{\rho_0} - 1 - u \right)^b + G_1(1-F)^c F^d p^e + G_2(1-F)^f F^g p^h \quad (3)$$

Where F is the fraction reacted, t the time, ρ the current density, ρ_0 the initial density, p the pressure, I , G_1 , G_2 , a , b , x , c , d , y , e , g and z are constants. For the ZND model of detonation, the first term in the right hand side of the formula denotes the part of explosives ignited by shock, the second term denotes the fast reaction of explosives, the last term denotes the reaction after the CJ point. For the aluminized explosives detonation, the last term denotes the aluminum oxidation reaction with the detonation products.

5. Results and discussions

In the cylinder tests, the displacements versus time of the cylinder expansion were measured by the rotating mirror streak camera. The wall velocities of the 25mm cylinder were measured by the VISAR interferometer.

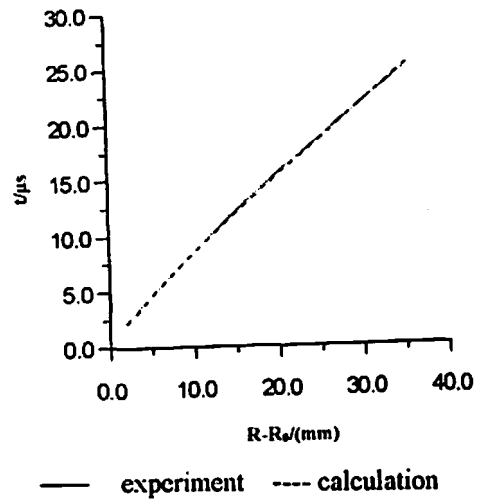


Fig. 4 Experimental and calculated displacements versus time of 50mm cylinder expansion with RDX/Al(5 μ m) mixtures

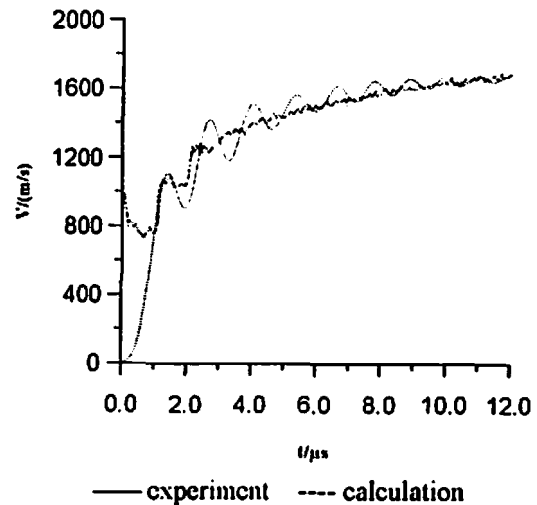


Fig. 5 Experimental and calculated wall velocity histories of 25mm cylinder expansion with RDX/Al (5 μ m) mixtures

In the calculations, the parameters of JWL equations of state were adjusted to the group of data until the calculated displacements versus time of the cylinder expansion are in good agreement with the experimental results. Figure 4 illustrates the comparison of the experimental and the finally calculated displacements versus time of the 50mm cylinder expansion with RDX/Al (5 μ m) mixtures.

Table 2 Fitted parameters of JWL equations of state

A/(100GPa)	B/(100GPa)	C/(100GPa)	R ₁	R ₂	ω
7.520	0.120	0.01253	4.4	1.3	0.33

Table 3 Parameters of the ignition and growth reactive flow model of aluminized explosives with different aluminum particle size.

Size	I × 10 ⁷	b	a	x	G ₁ × 10 ²	c	d	y	G ₂	e	g	z
50nm	6.0	0.667	0.11	10	2	1.0	1.0	1.0	11	1.0	1.0	1.0
5μm	6.0	0.667	0.11	10	2	1.0	1.0	1.0	8	1.0	1.0	1.0
50μm	6.0	0.667	0.11	10	2	1.0	1.0	1.0	6	1.0	1.0	1.0

Table 2 shows the fitted parameters of JWL equations of state.

With the parameters in Table 2, the wall velocity histories of the cylinder expansion may be calculated. Figure 5 compares the wall velocity histories of 25mm cylinder measured by the VISAR interferometer with the calculated wall velocity histories of 25mm cylinder for RDX/Al(5μm) mixtures. The average of the calculated velocity agrees with the VISAR velocity. It shows that the experimental results of the VISAR interferometer agree with those by the rotating mirror streak camera.

In the simulations of the metal plates push tests, the results of the experiments are compared with that of the calculations. The parameters of the ignition and growth reactive flow model are determined by more than one calculation.

Table 3 shows the three groups of the parameters of aluminized explosives with different aluminum particle sizes.

It is shown in Table 3 that for the three aluminized explosives, the all parameters are the same except G₂.

Figure 6~11 show the comparison of the experimental and calculated velocity histories of 1mm and 0.5mm copper plates driven by the three aluminized explosives respectively. In each figure, the two curves are in good agreement in reasonable range. That shows the parameters in Tables 2 and 3 are valid for the aluminized explosives.

In C-J detonation model, it is supposed that the explosives are reacted completely at C-J point. For the aluminized explosives, the calculated results with C-J model are that there are no reactions after the C-J point. Figure 12 gives the comparison of the calculated velocities history of 1mm copper plate between the CJ model and the ignition and

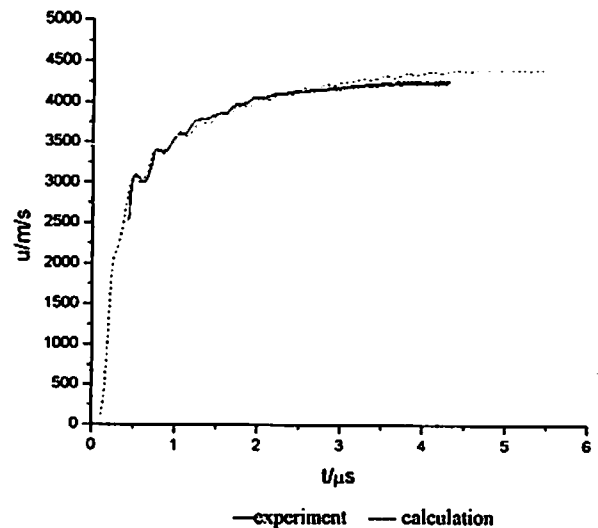


Fig. 6 Experimental and calculated velocity histories of 0.54mm copper plates driven by RDX/Al(5nm) mixtures

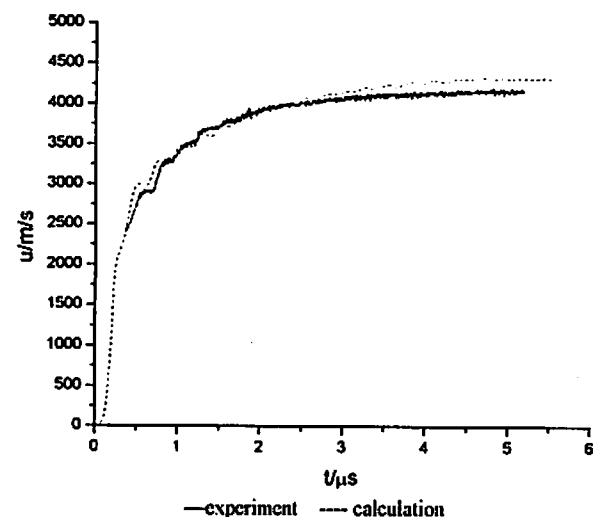


Fig. 7 Experimental and calculated velocity histories of 0.54mm copper plates driven by RDX/Al(5μm) mixtures

growth reactive flow model. The velocities of the copper plate calculated with the two models are the same in the first time, but the surface velocities

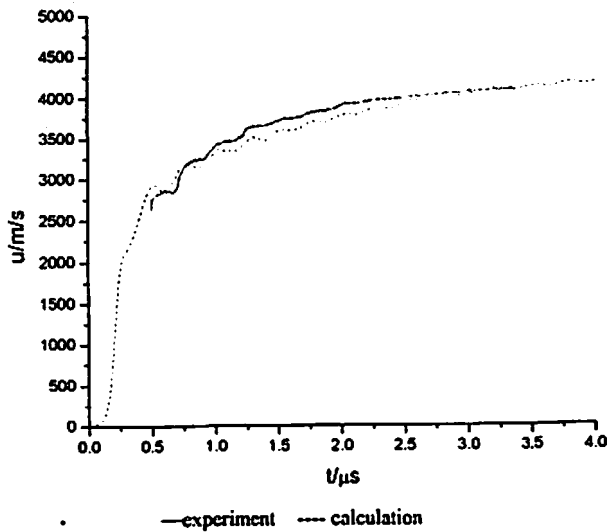


Fig. 8 Experimental and calculated velocity histories of 0.54mm copper plates driven by RDX/Al(50 μ m) mixtures

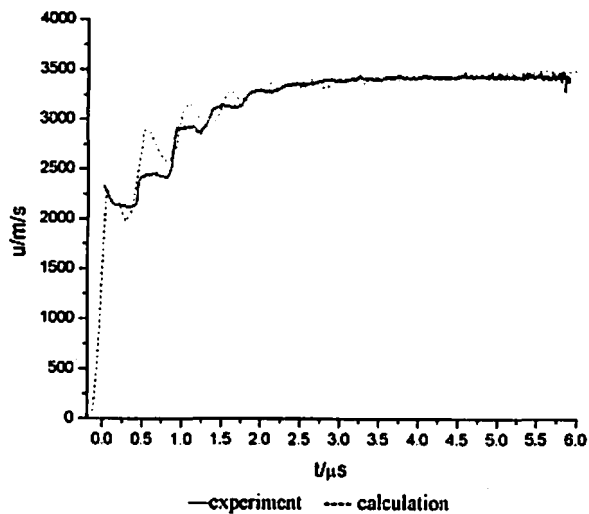


Fig. 9 Experimental and calculated velocity histories of 1mm copper plates driven by RDX/Al(50 μ m) mixtures

of the copper plate calculated with the ignition and growth reactive flow model are faster than that with C-J model in the late time. The velocities of the copper plate calculated with the ignition and growth reactive flow model are shown to be in good agreement with the experimental results as stated before. It indicates some aluminum particles react after the C-J point.

To analyze the aluminum particles reaction, the fractions of reacted aluminized explosives in early time are calculated. Figure 13 is the calculated fraction of reacted aluminized explosives in the push tests. It can be seen that, with 5nm aluminum

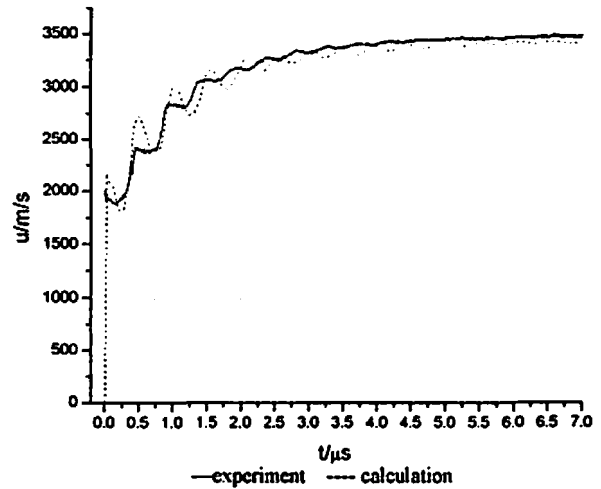


Fig. 10 Experimental and calculated velocity histories of 1mm copper plates driven by RDX/Al(5 μ m) mixtures

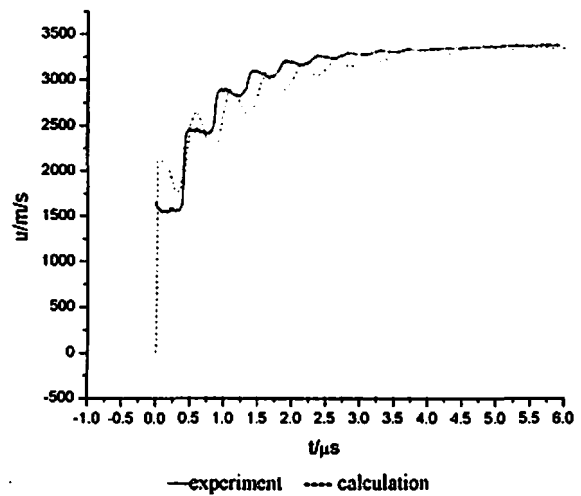


Fig. 11 Experimental and calculated velocity histories of 1mm copper plates driven by RDX/Al(50 μ m) mixtures

particles, the fraction reacted in 1mm copper plate test and in 0.5mm copper plate test are the same. The fraction reacted reached about 99% at 2.5 μ s. At 3.5 μ s, the fraction reacted is about 99% and does not change after the time. The time agrees basically to the 3.6 μ s that is the accelerated time of the copper plates.

For accelerating the 0.54mm and 1mm coppers, the fraction of reacted explosives with 50 μ m aluminum particles reached 99% and 98%, the maximum value, in 4.5 μ s and 5.7 μ s, respectively. These times also agree to the 4.5 μ s and 5.7 μ s that are the accelerated time of the copper plates in metal plate push tests.

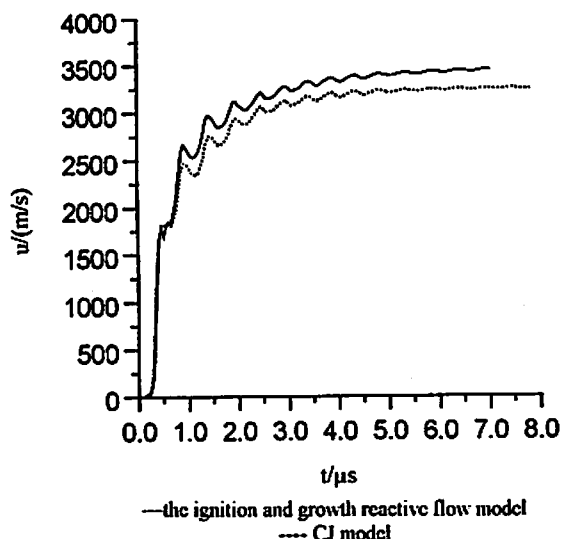


Fig. 12 Velocity histories of 1mm copper plates calculated with the ignition and growth reactive flow model and the JWL equations of state given in the present paper are available to the aluminized explosives with different sizes of aluminum particles.

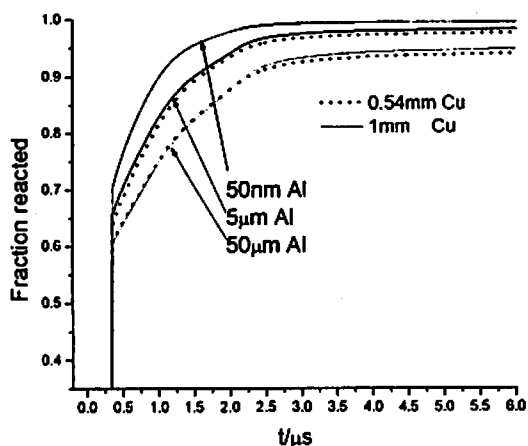


Fig. 13 Comparison of the reaction rate of explosives with different aluminum particle size in pushing 0.5mm copper and 1mm copper plate

It can be seen that a part of 50nm aluminum particles reacted in detonation waves since the explosives with 50nm aluminum particles have reacted 96% in 1.5 μ s. For the small size aluminum particles, the fraction of reacted explosives are higher than that of the large size at the same time. It shows the size of aluminum particles will affect the speed and time of aluminum oxidation reaction. The small size aluminum particles have larger surface areas and can mix easily with the detonation products to react fast.

To accelerate the 1mm copper plate, the fraction of reacted explosives with 5 μ m aluminum particles

or 50 μ m aluminum particles are higher than that of to accelerate the 0.5mm copper plate. It shows that the fraction of reacted explosives with large size aluminum particles depend on the confinement. The strong confinement will keep the detonation products in relative high pressure for longer time to let the aluminum particles react faster and more completely. For the small size aluminum particles, such as the 5nm aluminum particles, the reactions do not depend on confinement of explosives.

6 Conclusions

The calculated results are in good agreement with the experimental results. The ignition and growth reactive flow model and the JWL equations of state given in the present paper are available to the aluminized explosives with different sizes of aluminum particles. The large size aluminized particles react with products and release energy at late time in the detonation. The strong confinement of explosives will accelerate the reaction. The small size aluminum particles, such as 50nm aluminum particles, react mostly in the detonation waves and their reactions do not depend on the confinement of explosives.

References

- 1) M. Finger, H.C. Horning, E. L. Lee, and J. W. Kury, "Metal Acceleration by Composite Explosives", in Fifth Symposium (International) on Detonation (Office of Naval Research Report ACR-184, August 1970) pp.137(1970)
- 2) G. B. Jarnholt, "Effects of Aluminum and Lithium Flouride Admixtures on Metal Acceleration Ability of Comp B", in Sixth Symposium(International) on Detonation (Office of Naval Research Report ACR-221, August 1976) ,pp.510 (1976)
- 3) W. C. Tao, C. M. Tarver, J. W. Kury, C.G.Lee and D. L. Ornellas, "Understanding Composite Explosive Energetics: IV. Reactive Flow Modeling of Aluminum Reaction Kinetics in Pent and TNT Using Normalized Product Equation of State". Tenth Symposium (International) on Detonation, pp.628-636. (1993)

- 4) G. Baudin and D. Bergues, "A Reaction Model for Aluminized PBX Applied to Underwater Explosive Calculations". Tenth Symposium (International) on Detonation, pp.646-655 (1993).
- 5) R. H. Guiruis and P. J. Miller, "Time-Dependent Equations of State for Aluminized Underwater Explosives". Tenth Symposium (International) on Detonation, pp.675-682. (1993)
- 6) X. P. Long. The VLW Equation of State for Detonation Products and the Detonation Characteristics of Nanometer Aluminized Explosives. PhD thesis. Beijing Institute of Technology. Beijing, China, 1999.
- 7) C. M. Tarver JO, Hallquist, L. M. Erickson, "Modeling of short pulse duration shock initiation of solid explosives", 8th Symposium (International) on Detonation. White Oak, Silver Spring, Maryland: Naval Surface Weapons Center, 884 (1986)

